

See discussions, stats, and author profiles for this publication at: <https://www.researchgate.net/publication/260991774>

# Experimental and Modeling Study on Ignition Delay Times of Dimethyl Ether/n-Butane Blends at a Pressure of 2.0 MPa

ARTICLE in ENERGY & FUELS · MARCH 2014

Impact Factor: 2.79 · DOI: 10.1021/ef402277h

CITATIONS

3

READS

23

5 AUTHORS, INCLUDING:



Shaodong Niu

51 PUBLICATIONS 253 CITATIONS

SEE PROFILE



Lun Pan

University of Wisconsin-Madison

46 PUBLICATIONS 126 CITATIONS

SEE PROFILE



Zuohua Huang

Xi'an Jiaotong University

421 PUBLICATIONS 5,195 CITATIONS

SEE PROFILE

# Experimental and Modeling Study on Ignition Delay Times of Dimethyl Ether/*n*-Butane Blends at a Pressure of 2.0 MPa

Xue Jiang, Yingjia Zhang,\* Xingjia Man, Lun Pan, and Zuohua Huang\*

State Key Laboratory of Multiphase Flow in Power Engineering, Xi'an Jiaotong University, Xi'an 710049, People's Republic of China

## S Supporting Information

**ABSTRACT:** In this study, the ignition delay times of dimethyl ether (DME)/*n*-C<sub>4</sub>H<sub>10</sub> fuel blends, neat DME, and neat *n*-C<sub>4</sub>H<sub>10</sub> diluted with argon were measured behind reflected shock waves. The experiments were performed in the temperature range of 1100–1600 K, at a pressure of 2.0 MPa, and equivalence ratios from 0.5 to 2.0. A latest kinetic mechanism NUIG Aramco Mech 1.3 was validated against the measured ignition data and used to conduct the chemical kinetic analysis. Results showed that different equivalence ratio-dependent behaviors were exhibited at different temperature regimes for DME, *n*-C<sub>4</sub>H<sub>10</sub>, and their blend. The ignition delay time of neat *n*-C<sub>4</sub>H<sub>10</sub> was increased with an increase in the equivalence ratio. A strong inhibiting trend was exhibited at high temperatures. For the neat DME, however, an opposite influencing tendency from the equivalence ratio was presented in comparison to that on *n*-C<sub>4</sub>H<sub>10</sub>. Ignition promotion becomes significant at relatively low temperatures. A 50% DME/50% *n*-C<sub>4</sub>H<sub>10</sub> blend show a combined behavior of both *n*-butane and DME. Fuel reaction flux analysis, sensitive analysis, and mole fraction analysis were conducted for the understanding of the interaction between the ignition chemistries of DME and *n*-C<sub>4</sub>H<sub>10</sub> at a pressure of 2.0 MPa.

## 1. INTRODUCTION

Alternative fuel has attracted increasing attention because of the issues of energy shortage and environmental pollution. Thus, use of efficient combustion technology and development of alternative fuels are the effective ways to tackle these issues. Homogeneous charge compression ignition (HCCI) is one of the clean combustion technologies because of its high thermal efficiency and extremely low emissions. It is well-known that ignition and combustion characteristics of a HCCI engine are mainly controlled by the fuel chemical kinetics; thus, reasonable fuel design is an effective approach to control the HCCI engine autoignition. A combination of fuels with high octane numbers and high cetane numbers can meet the requirement of different operations of HCCI.

Dimethyl ether (DME) is the simplest ether, which is a diesel alternative fuel with a high cetane number (55–60). It has a relatively low autoignition temperature. The high oxygen content and no C–C bond enable it to have soot-free combustion.<sup>1</sup> Lots of studies have been conducted on the fuel combination of high-octane-number fuel blended with DME. Dagaut et al.<sup>2,3</sup> studied the ignition and oxidation of DME in a spherical fused-silica jet-stirred reactor (JSR) over a wide range of pressures (1.0–10.0 atm), equivalence ratios (0.2 <  $\phi$  < 2.0), and temperatures (550–1300 K) and developed a kinetic mechanism for DME. Cook et al.<sup>4</sup> measured the ignition delay times and OH concentration time histories of argon-diluted DME and validated several kinetic models. Initial conditions covered the temperatures of 1175–1900 K, pressures of 1.6–6.6 bar, and equivalence ratios of 0.5–3.0. They found that the DME decomposition reaction and  $\text{H} + \text{O}_2 = \text{OH} + \text{O}$  were most important in the DME oxidation and directly measured the reaction rate of  $\text{DME} = \text{CH}_3\text{O} + \text{CH}_3$ . Pfahlet al.<sup>5</sup> studied the autoignition of DME/air using the shock tube at a high pressure (1.3 MPa) and intermediate–low

temperatures (840–1300 K) and observed a two-stage autoignition behavior in the ignition process of DME. Hidaka et al.<sup>6</sup> investigated the pyrolysis of DME using the shock tube over the temperature range of 900–1900 K and pressures of 0.83–2.9 atm. They evaluated the rate constant expressions of several key reactions and found that the tendency to form higher hydrocarbons (HCs) via the DME pyrolysis reaction was decreased at increased temperatures. Ji et al.<sup>7</sup> investigated the combustion and emissions of DME/gasoline mixtures in a four-cylinder spark-ignition engine at stoichiometric conditions. The DME fraction was varied from 0 to 30%. Experimental results showed that NO<sub>x</sub> and HC emissions reduce with DME addition. A small amount of DME (less than 10%) can improve the combustion performance. Jeon and Bae<sup>8</sup> studied the premixed charge compression ignition (PCCI) combustion characteristics of the DME and hydrogen blend using a compression ignition engine. They suggested that the start of combustion was determined by the DME injection timing. Meanwhile, the exhaust emissions were decreased with the addition of hydrogen. Additionally, Tsutsumi et al.<sup>9</sup> and Konno et al.<sup>10</sup> investigated the effects of DME/methane blends on the ignition timing and rapidity of combustion using a HCCI engine. Their results showed that the ignition kinetic of DME played the dominant role in the controlling of ignition timing, but the rapidity of combustion was not effectively controlled by the mixing ratios of DME and methane.

*n*-Butane (*n*-C<sub>4</sub>H<sub>10</sub>) is one of the main components of natural gas. It has a high octane number (about 91.8). Iida et al.<sup>11–13</sup> conducted a series of experimental and numerical studies on combustion and emission characteristics of DME/

Received: November 18, 2013

Revised: February 19, 2014

Published: February 19, 2014

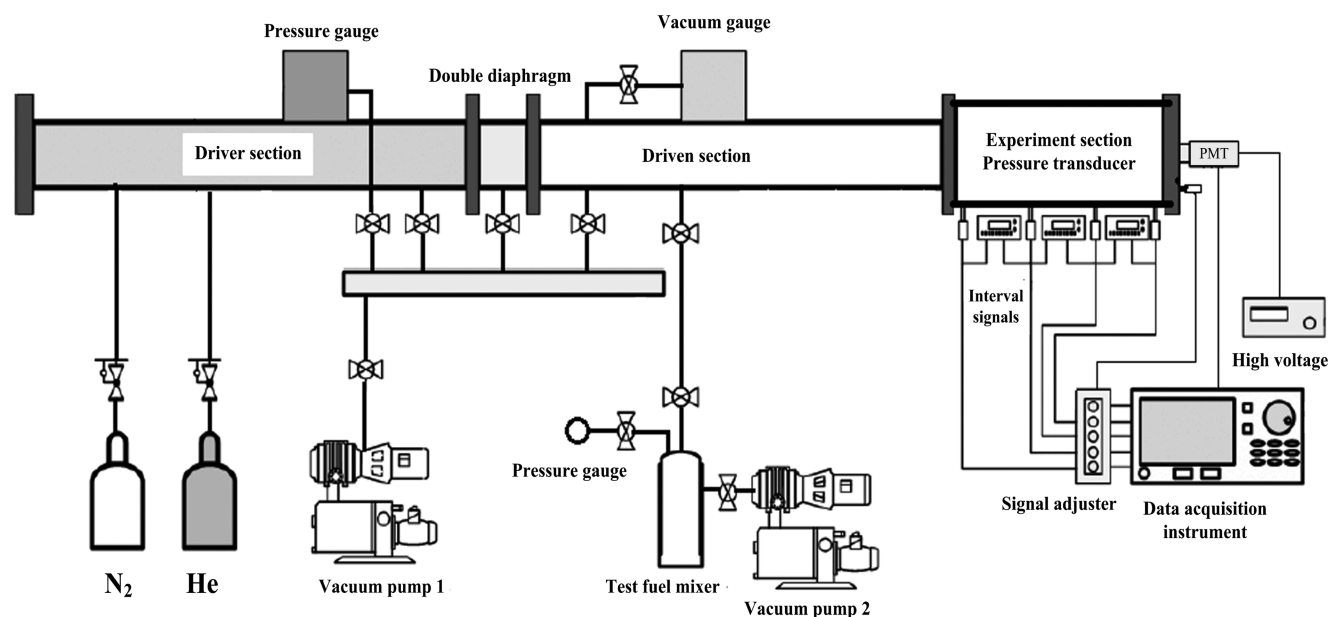


Figure 1. Schematic of the shock tube.

HC fuel blends under the operating conditions of a HCCI engine. The tested HC fuels included methane, propane, and *n*-butane. Healy et al.<sup>14</sup> measured the ignition delay time of *n*-butane using both a shock tube and rapid compression machine at equivalence ratios of 0.3, 0.5, 1.0, and 2.0 and pressures of 1.0, 10, 20, 30, and 45 atm. They developed a kinetic model of *n*-butane against the measured data. Their developed model can well-reproduce both experimental observation and other data in the literature. Zhang et al.<sup>15</sup> measured the ignition delay times of the stoichiometric mixtures of C<sub>1</sub>–C<sub>4</sub> alkanes (methane, ethane, propane, and *n*-butane) behind reflected shock waves. Experiments were carried out at pressures of 1.2 and 5.3 atm and the temperature range of 1100–2100 K. The study revealed that methane gave the longest ignition delay time, while ethane showed the shortest ignition delay time. The ignition delay times of propane and *n*-butane are between methane and ethane. Furthermore, a previous study reported that *n*-butane and isobutane demonstrated the two-stage ignition and obvious negative temperature coefficient (NTC) ignition behavior at low temperatures.<sup>16</sup> This behavior is similar to that of DME.

For the autoignition characteristics of DME/*n*-C<sub>4</sub>H<sub>10</sub> blends, up to now, only two available studies were reported. Hu et al.<sup>17</sup> measured the ignition delay times of the stoichiometric DME/*n*-C<sub>4</sub>H<sub>10</sub> blends with varied DME blending ratios (0, 30, 70, and 100%) at high temperatures (1200–1600 K) and relatively low pressures (0.12–0.53 MPa). They found that the addition of DME could significantly promote the ignition process of *n*-C<sub>4</sub>H<sub>10</sub>. However, the latest study on ignition delay times of lean DME/*n*-C<sub>4</sub>H<sub>10</sub> conducted under pressures of 0.2–2.0 MPa, temperatures from 1100 to 1600 K, and DME blending ratios from 0 to 100% reported that an increase of the pressure could also significantly promote the ignition but the ignition delay time of *n*-butane was considerably insensitive to the change of the DME blending ratio.<sup>18</sup>

The ignition delay times of DME/*n*-C<sub>4</sub>H<sub>10</sub> blends at a high pressure are important to the HCCI engine ignition control as well as the development of the kinetic mechanism. However, the measurements on the ignition delay time of DME/*n*-C<sub>4</sub>H<sub>10</sub>

fuel blends at a high pressure and various equivalence ratios are still lacking. To further understand the effect of equivalence ratios on fuel ignition characteristics, it is necessary to study and provide the ignition delay times of DME/*n*-C<sub>4</sub>H<sub>10</sub> blends at an engine-relevant pressure with different equivalence ratios. Thus, one objective of this study is to measure the ignition delay times of DME/*n*-C<sub>4</sub>H<sub>10</sub> blends at a high pressure and wide equivalence ratios. Another purpose is to identify the dominant reactions and then clarify the enhancing and inhibiting effects on the autoignition with the variation of the equivalence ratio through chemical kinetic analysis.

## 2. EXPERIMENTAL SECTION

**2.1. Experimental Setup.** Measurements were conducted in a high-pressure stainless shock tube, and all experiments were performed in a shock tube, which has been described in details in previous publications.<sup>19,20</sup> The schematic of the shock tube is shown in Figure 1. This shock tube with an internal diameter of 11.5 cm is separated into a 2 m long driver section and a 7.3 m long driven section by double polyester terephthalate (PET) diaphragms. A Nanguang vacuum system evacuated the pressure of the driven section below 1.0 Pa. High-purity helium and nitrogen mixtures were used as driver gas. The CH\* chemiluminescence was selected by a narrow filter centered at 430 ± 10 nm and detected through a photomultiplier (Hamamatsu, CR131) located at the endwall. Incident shock velocity at the endwall was determined by linear extrapolation using four fast-response piezoelectric pressure transducers (PCB 113B26) with three time interval counters (Fluke PM6690) located at fixed intervals along the driven section. The temperature and pressure behind the reflected shock wave were calculated by chemical equilibrium software Gaseq.<sup>21</sup> The typical uncertainty of the temperature is ±15 K based on contributions from random and systematic uncertainties of time interval counters and the measurement error of distances between pressure transducers.<sup>19</sup>

The ignition delay time is defined as the time interval between the arrival of the incident shock wave at the endwall and the extrapolation of the steepest rise of CH\* chemiluminescence to the zero baseline, as shown in Figure 2. Test mixtures were prepared in a 128 L stainless-steel tank and allowed to settle 12 h to ensure sufficient mixing. Fuel mixtures were prepared according to Dalton's partial pressure law mentioned in the previous studies.<sup>19,22</sup> The fuel/oxygen/argon mixture ( $\phi = 0.5, 1.0, \text{ and } 2.0$ ; [O<sub>2</sub>]/[Ar] = 21/79% as air) was

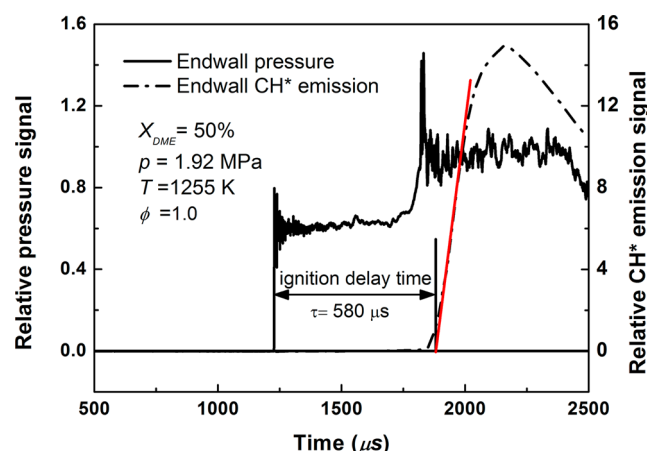


**Figure 2.** Ignition delay time measurement from endwall pressure and CH\* emission.

diluted with argon (20% mixture/80% Ar). All fuel mixtures were diluted with an identical dilution ratio. Purities of DME, *n*-butane, oxygen, and argon are higher than 99.999%. The detail components of test mixtures are shown in Table 1.

**Table 1.** Composition of Fuel Mixtures

mixture	$\phi$	$X_{\text{DME}}$ (%)	$X_{\text{C}_4\text{H}_{10}}$ (%)	$X_{\text{O}_2}$ (%)	$X_{\text{Ar}}$ (%)
100% DME	0.5	0.676	0.000	4.056	95.268
50% DME/50% <i>n</i> -C <sub>4</sub> H <sub>10</sub>	0.5	0.216	0.216	4.105	95.463
100% <i>n</i> -C <sub>4</sub> H <sub>10</sub>	0.5	0.000	0.318	4.134	95.548
100% DME	1	1.308	0.000	3.924	94.768
50% DME/50% <i>n</i> -C <sub>4</sub> H <sub>10</sub>	1	0.423	0.423	4.019	95.135
100% <i>n</i> -C <sub>4</sub> H <sub>10</sub>	1	0.000	0.626	4.069	95.305
100% DME	2	2.456	0.000	3.684	93.860
50% DME/50% <i>n</i> -C <sub>4</sub> H <sub>10</sub>	2	0.812	0.812	3.857	94.519
100% <i>n</i> -C <sub>4</sub> H <sub>10</sub>	2	0.000	1.214	3.945	94.841

**2.2. Kinetic Simulation.** Simulations were made using the SENKIN code<sup>23</sup> of the CHEMKIN II program<sup>24</sup> and the NUIG Aramco Mech 1.3 mechanism.<sup>25</sup> This mechanism was developed by the Combustion Chemistry Center at the National University of Ireland in 2013, which consists of 253 chemical species and 1542 elementary reactions. The Aramco Mech 1.3 mechanism can describe the kinetic properties of the saturated HCs, unsaturated HCs, and oxygenated species. This mechanism has been widely validated by the flow reactor, jet-stirred reactor, shock tube, and flame. The zero-dimensional and constant volume adiabatic model was adopted in the simulation. In the simulation, the initial pressure was set to a fixed value of 2.0 MPa, and the initial temperature (i.e., reflected shock temperature) variation ranges from 800 to 1800 K, with temperature step of 25 K. The  $t = 0$  moment was defined as the arrival of the incident shock wave at the endwall. In this study, an obvious pressure rise ( $dp/dt = 4\%/ms$ ) was experimentally observed because of the interaction between the reflected shock wave and boundary layer, especially for the longer ignition time.<sup>18,19</sup> Because the non-ideal effect significantly influences the prediction of the ignition delay time, the pressure rise was taken into account in the numerical simulations.

### 3. RESULTS AND DISCUSSION

Ignition delay times of neat *n*-C<sub>4</sub>H<sub>10</sub>, neat DME, and DME/*n*-C<sub>4</sub>H<sub>10</sub> blends were measured at equivalence ratios of 0.5, 1.0, and 2.0 and a pressure of 2.0 MPa. All measured ignition delay times are summarized in the Supporting Information and are also presented in Figures 3 and 4.

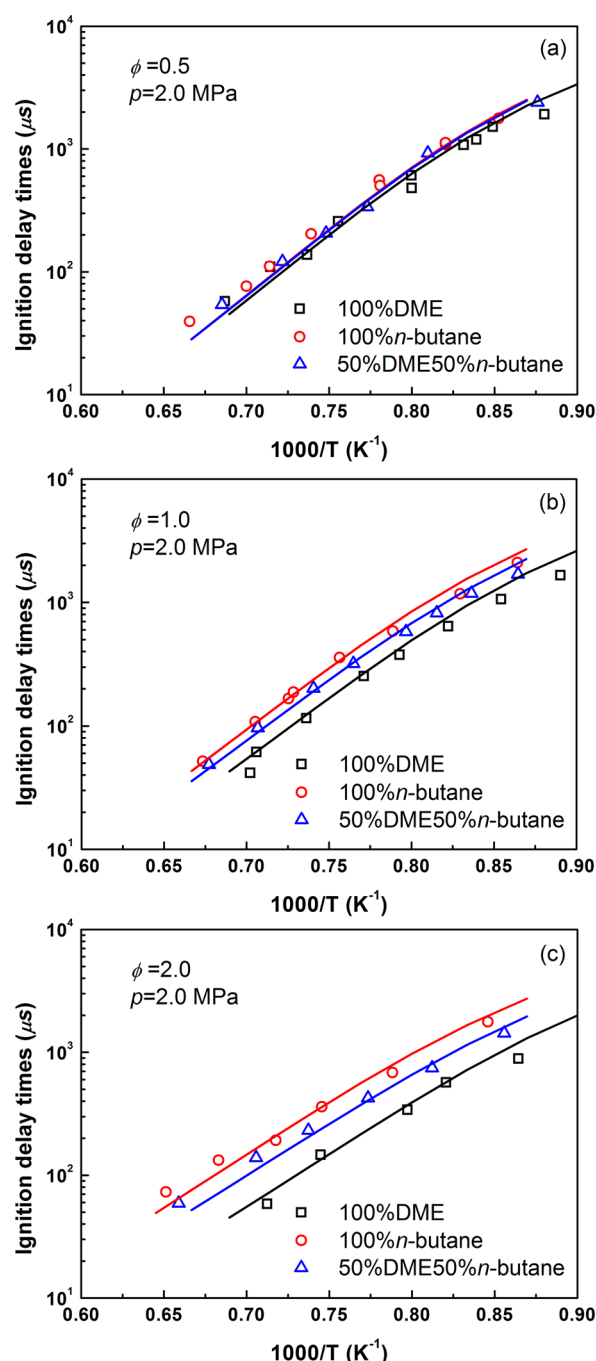


**Figure 3.** Effects of DME blending at different equivalence ratios: (a)  $\phi = 0.5$ , (b)  $\phi = 1.0$ , and (c)  $\phi = 2.0$  (symbols, experiment; lines, simulation using NUIG Aramco Mech 1.3).

**3.1. Effect of DME Addition.** Figure 3 shows the effects of DME addition on the ignition delay times of *n*-butane at different equivalence ratios. In general, the experimental data exhibit good agreement with the simulated results. It is noted that, under the fuel-lean condition ( $\phi = 0.5$ ), the ignition delay times of neat DME, neat *n*-C<sub>4</sub>H<sub>10</sub>, and DME/*n*-C<sub>4</sub>H<sub>10</sub> mixtures are almost the same, suggesting an insensitive equivalence ratio dependency of the ignition delay time upon the DME blending. This observation is consistent with that in the previous study by the authors.<sup>18</sup> However, under the fuel-stoichiometric ( $\phi = 1.0$ ) and fuel-rich ( $\phi = 2.0$ ) conditions, the effects of DME blending are obvious, especially under the fuel-rich conditions. DME



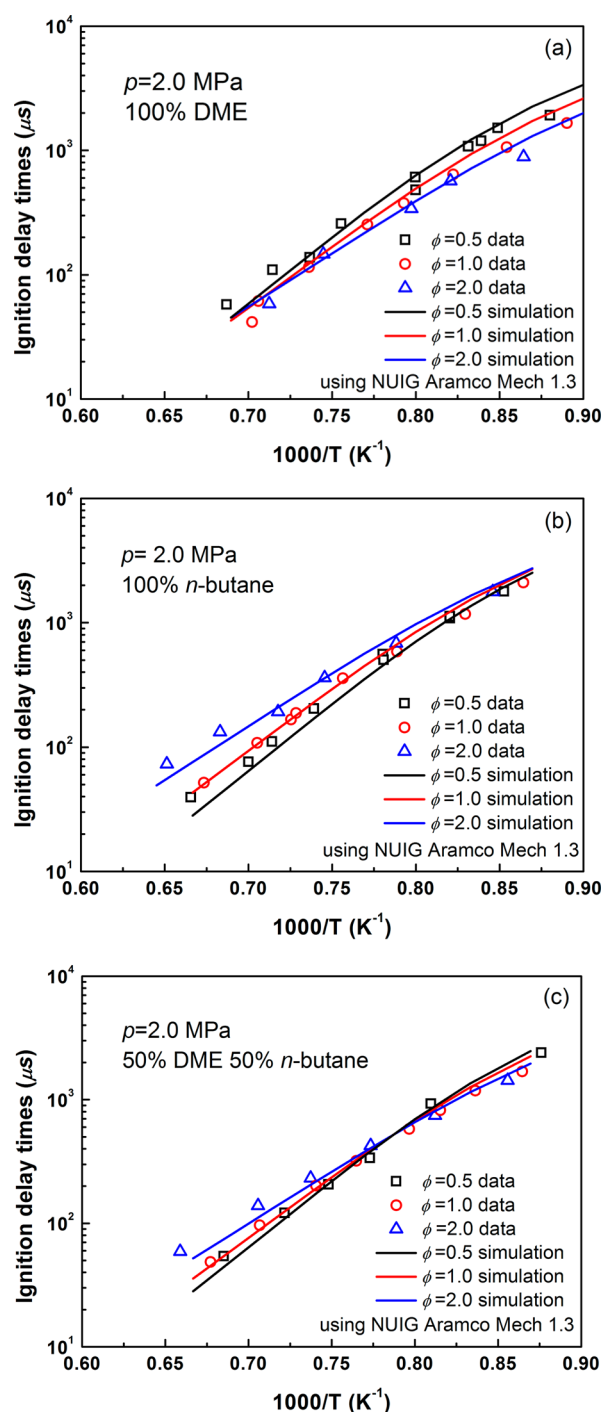


**Figure 4.** Measured and simulated ignition delay times of DME, *n*-butane, and their blends at various equivalence ratios: (a) neat DME, (b) neat *n*-butane, and (c) 50% DME/50% *n*-butane (symbols, experiment; lines, simulation using NUIG Aramco Mech 1.3).

addition can significantly promote the ignition of *n*-butane. Neat DME gives the shortest ignition delay times, while neat *n*-butane gives the longest ignition delay times. The addition of DME can promote the ignition process of *n*-C<sub>4</sub>H<sub>10</sub>, and this observation agrees well with the study by Hu et al.<sup>17</sup> It is noted that DME addition does not change the global activation energy of *n*-butane at three equivalence ratios.

**3.2. Effect of the Equivalence Ratio.** Figure 4 shows the effect of the equivalence ratio on the ignition delay times of neat *n*-C<sub>4</sub>H<sub>10</sub>, neat DME, and DME/*n*-C<sub>4</sub>H<sub>10</sub> blends at an

engine relevant pressure. The ignition delay times simulated by the NUIG Aramco Mech 1.3 mechanism are also plotted in this figure for comparison. The results show excellent agreement between model simulation and measured ignition delay times under all investigated conditions. For the neat DME, as shown in Figure 4a, all mixtures at different equivalence ratios give almost the same ignition delay times at the highest temperature (approximately 1470 K). However, the effect of the equivalence ratio on autoignition becomes considerably significant with the decrease of the temperature. In this case, both experiment and simulation exhibit shorter ignition delay times under the fuel-rich conditions, meaning that the ignition delay time of DME decreases with an increase of the equivalence ratio. Cook et al.<sup>4</sup> found that, for neat DME, a fuel-rich mixture exhibited longer ignition delay times than a fuel-lean mixture under high-temperature conditions. The differences from those of the current study are mainly caused by the differences in pressure and component of the test mixtures. For *n*-C<sub>4</sub>H<sub>10</sub>, as shown in Figure 4b, the influencing tendency of the equivalence ratio on the ignition delay times is just opposite that of DME. All mixtures exhibit the same ignition delay times at the lowest temperature (approximately 1150 K). Moreover, the fuel-lean mixture presents the shortest ignition delay time, while the fuel-rich mixture exhibits the longest ignition delay time, indicating that the ignition delay times increase with the increase of the equivalence ratio. It is also observed that the influencing extent from the equivalence ratio becomes gradually strong with the increase of the temperature. For the 50% DME/50% *n*-C<sub>4</sub>H<sub>10</sub> mixture, as shown in Figure 4c, a similar behavior to that of neat *n*-C<sub>4</sub>H<sub>10</sub> is presented in the high-temperature range ( $T > 1250$  K). An increasing equivalence ratio can inhibit the ignition and increase the ignition delay times. Ignition delay times show a similar tendency to that of the neat DME in a relatively low-temperature range ( $T < 1250$  K), and the fuel-rich mixture gives the shortest ignition delay time. This indicates the dominating role of *n*-butane chemistry on the ignition kinetics of the 50% DME/50% *n*-butane mixture at high temperatures, and DME chemistry dominates the ignition kinetics at the low-temperature range. For the 50% DME/50% *n*-C<sub>4</sub>H<sub>10</sub> mixtures, there is a crossing point of ignition delay times under different equivalence ratios at  $T = 1250$  K. As a result, the ignition delay time is considerably insensitive to the variation of equivalence ratios in this case.

## 4. CHEMICAL KINETIC ANALYSIS

**4.1. Fuel Flux Analysis.** Reaction flux analysis on neat DME and neat *n*-C<sub>4</sub>H<sub>10</sub> fuels was performed using NUIG Aramco Mech 1.3, as shown in Figures 5 and 6. Analysis was made at equivalence ratios of 0.5, 1.0, and 2.0, a pressure of 2.0 MPa, and temperatures of 1150 and 1550 K. A snapshot of the reaction flux of 20% fuel consumption is provided similar to that in the literature.<sup>26</sup>

For neat DME (Figure 5), the scheme shows that, regardless of the temperature, fuel is mainly consumed via the H-abstraction reaction and produces the methoxymethyl radical (CH<sub>3</sub>OCH<sub>2</sub>). This amount accounts for more than 94% of the total fuel consumption at a higher temperature (1550 K), while the percentage reduces to about 72% at a lower temperature (1150 K). Subsequently, all of the formed methoxymethyl radical (CH<sub>3</sub>OCH<sub>2</sub>) is decomposed to form the methyl radical and formaldehyde (CH<sub>2</sub>O). Meanwhile, a small amount of DME undergoes an unimolecular decomposition reaction to produce the methoxyl radical (CH<sub>3</sub>O) and methyl radical. The

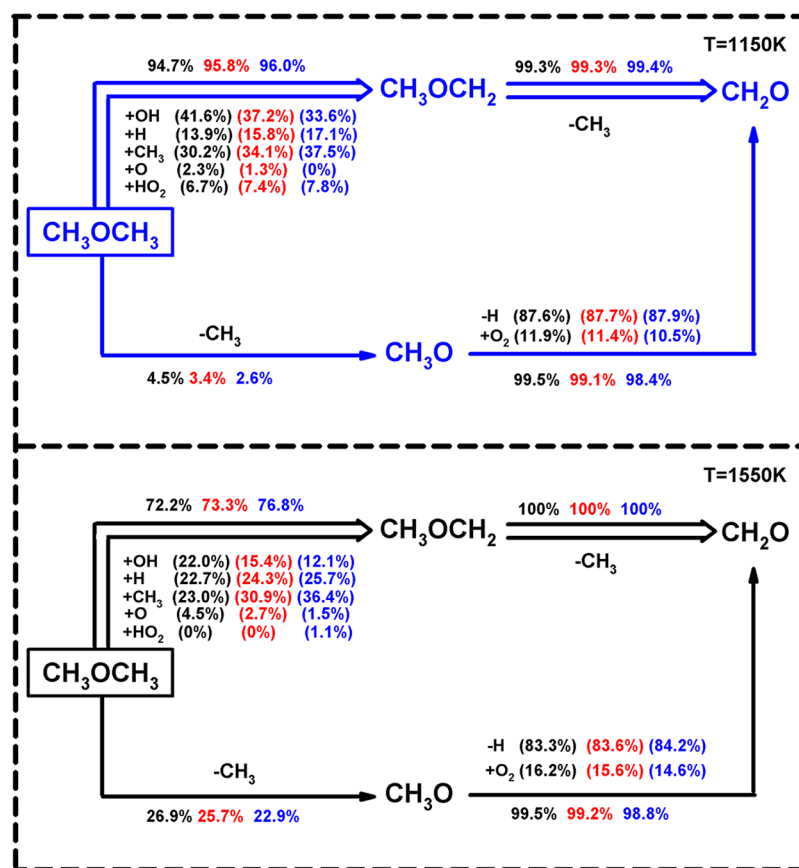


**Figure 5.** Reaction pathway diagram for DME in the shock tube at  $p = 2.0$  MPa,  $T = 1550$  K, and 20% DME consumption using NUIG Aramco Mech 1.3 (black,  $\phi = 0.5$ ; red,  $\phi = 1.0$ ; and blue,  $\phi = 2.0$ ).

relatively unstable methoxyl radical loses a hydrogen atom through either direct reaction with molecular oxygen or H-elimination reaction to form CH<sub>2</sub>O. The reaction pathway proportion of DME via the decomposition reaction is increased with the increase of the temperature.

A difference in fuel reaction flux was analyzed for the neat DME at two temperatures (1150 and 1550 K). At a relatively low temperature, DME mainly undergoes the H-abstraction reactions. While at a high temperature, a large percentage of DME consumption undergoes direct pyrolysis to form CH<sub>3</sub> and CH<sub>3</sub>O radicals, except the H-abstraction reaction. When the temperature increases from 1150 to 1550 K, the percentage of DME pyrolysis increases from 4.6 to 27%. The H-abstraction reactions always keep the dominant position in initial DME consumption, mainly through H, OH, and CH<sub>3</sub> and small contributions from O and HO<sub>2</sub>. At both temperatures, the percentages of the H-abstraction reaction through OH and O radicals are decreased, while those through CH<sub>3</sub>, H, and HO<sub>2</sub> radicals are increased with the increase of the equivalence ratio. Proportions of other small radicals contributing to the reactions are also varied with the variation of the equivalence ratio.

For neat  $n$ -C<sub>4</sub>H<sub>10</sub>, as shown in Figure 6, most  $n$ -C<sub>4</sub>H<sub>10</sub> undergo the H-abstraction reaction to produce the *sec*-butyl radical (SC<sub>4</sub>H<sub>9</sub>) and *n*-butyl radical (PC<sub>4</sub>H<sub>9</sub>). Because primary hydrogen atoms have higher bond dissociation energy (101.5 kcal/mol) than that of secondary hydrogen atoms (98.5 kcal/mol), more *sec*-butyl radicals (SC<sub>4</sub>H<sub>9</sub>) are formed compared to *n*-butyl radicals (PC<sub>4</sub>H<sub>9</sub>).<sup>27</sup> The proportion to form the SC<sub>4</sub>H<sub>9</sub> radical accounts for about 58% of the total  $n$ -C<sub>4</sub>H<sub>10</sub> consumption at a relatively low temperature (1150 K), and

the value is about 41% at a higher temperature (1550 K). OH and H radicals play the dominant role, while O, CH<sub>3</sub>, and HO<sub>2</sub> radicals have a small contribution at higher temperatures. Subsequently, most SC<sub>4</sub>H<sub>9</sub> form the propene (C<sub>3</sub>H<sub>6</sub>) and CH<sub>3</sub> radical via  $\beta$ -scission reactions. Simultaneously, approximate 30%  $n$ -C<sub>4</sub>H<sub>10</sub> forms the PC<sub>4</sub>H<sub>9</sub> radical through the H-abstraction reaction at  $T = 1150$  K, while this percentage decreases to 25% at  $T = 1550$  K. All PC<sub>4</sub>H<sub>9</sub> undergo the direct decomposition reaction to yield the ethyl radical (C<sub>2</sub>H<sub>5</sub>) and ethylene (C<sub>2</sub>H<sub>4</sub>). Furthermore, a small amount of  $n$ -C<sub>4</sub>H<sub>10</sub> is directly decomposed to form the propyl radical (NC<sub>3</sub>H<sub>7</sub>) through the C–C bond dissociation. NC<sub>3</sub>H<sub>7</sub> is then consumed by  $\beta$ -scission reactions to form the C<sub>2</sub>H<sub>4</sub> radical. A small percentage of  $n$ -C<sub>4</sub>H<sub>10</sub> also produces the C<sub>2</sub>H<sub>5</sub> radical through the directed composition reaction.

Particularly, at 1550 K, the H-abstraction reaction of  $n$ -C<sub>4</sub>H<sub>10</sub> dominates the initial consumption of fuel, in which the reaction with H radicals plays a major role. With the increase of the equivalence ratio, the percentage of the H radical contributing to PC<sub>4</sub>H<sub>9</sub> radical formation increases from 16.5 to 18.9%. For SC<sub>4</sub>H<sub>9</sub>, the H-abstraction reaction by the H radical accounts for 32.3% under fuel-rich conditions, higher than that under fuel-lean conditions (27.9%). It is well-known that H, O, OH, and HO<sub>2</sub> radicals are important free radicals to fuel consumption, among which H radicals give the most remarkable activity at high temperatures. The fuel concentration is increased with increasing the equivalence ratio; thus, more H radicals will be consumed by fuel via the H-abstraction reactions, and this leads to the decrease of total active free radicals in the radical pool. As a result, ignition delay times are increased with the increase

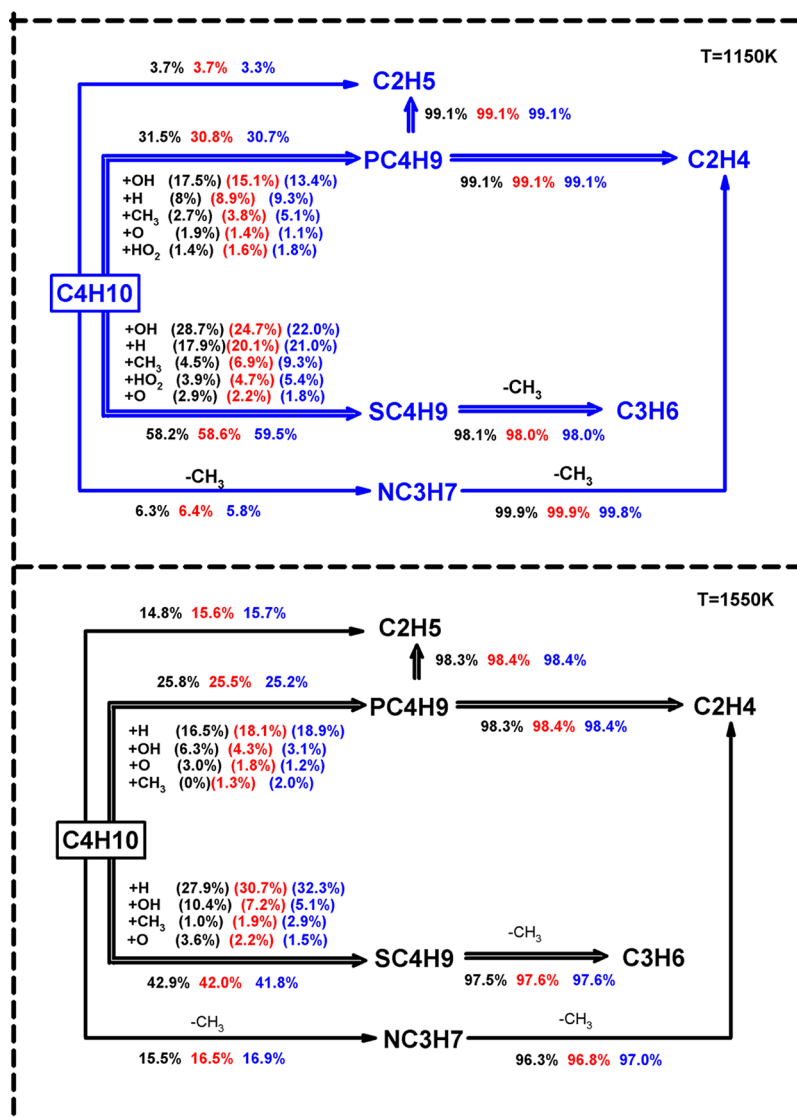


**Figure 6.** Reaction pathway diagram for *n*-butane in the shock tube at  $p = 2.0$  MPa,  $T = 1550$  K, and 20% *n*-butane consumption using NUIG Aramco Mech 1.3 (black,  $\phi = 0.5$ ; red,  $\phi = 1.0$ ; and blue,  $\phi = 2.0$ ).

of the equivalence ratio. The analysis is consistent with the experimental measurement in Figure 4b.

**4.2. Sensitivity Analysis.** Sensitivity analysis was made to identify the most important reactions in the ignition kinetics of DME/*n*- $C_4H_{10}$  blends. The normalized sensitivity of the ignition delay time was made at the same temperature as that for the fuel reaction flux analysis. The sensitivity coefficient is defined as

$$S = \frac{\tau(2k_i) - \tau(0.5k_i)}{1.5\tau(k_i)} \quad (1)$$

where  $\tau$  is the ignition delay time and  $k_i$  is the specific rate coefficient. Reactions with a positive coefficient inhibit the reactivity, while those with a negative coefficient promote the reactivity. In this study, NUIG Aramco Mech 1.3 was used to calculate the sensitivity coefficients. Figure 7 displays the sensitivity coefficients of neat DME at 1150 K, neat *n*- $C_4H_{10}$  at 1550 K, and DME/*n*- $C_4H_{10}$  fuel blends at 1150 and 1550 K at 2.0 MPa.

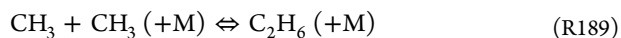
For neat DME at 1150 K, as shown in Figure 7a, reaction R437



which is the fuel-molecule-related H-abstraction reaction by the  $CH_3$  radical, is the most important promoting reaction. Moreover, the exothermic reaction R75



is another important promoting reaction. Through reaction R75, a relatively stable  $CH_3$  radical is consumed and a high-reactivity HCO is formed. Sensitivity coefficients of reactions R437 and R75 both increase with the increase of the equivalence ratio. This is because the concentrations of both DME and  $CH_3$  radicals are remarkably increased with the increase of the equivalence ratio, resulting in the increase of the ignition promoting tendency with the increase of the equivalence ratio. In contrast to these, the reactions with highest positive sensitivity coefficients are reactions R189 and R145.



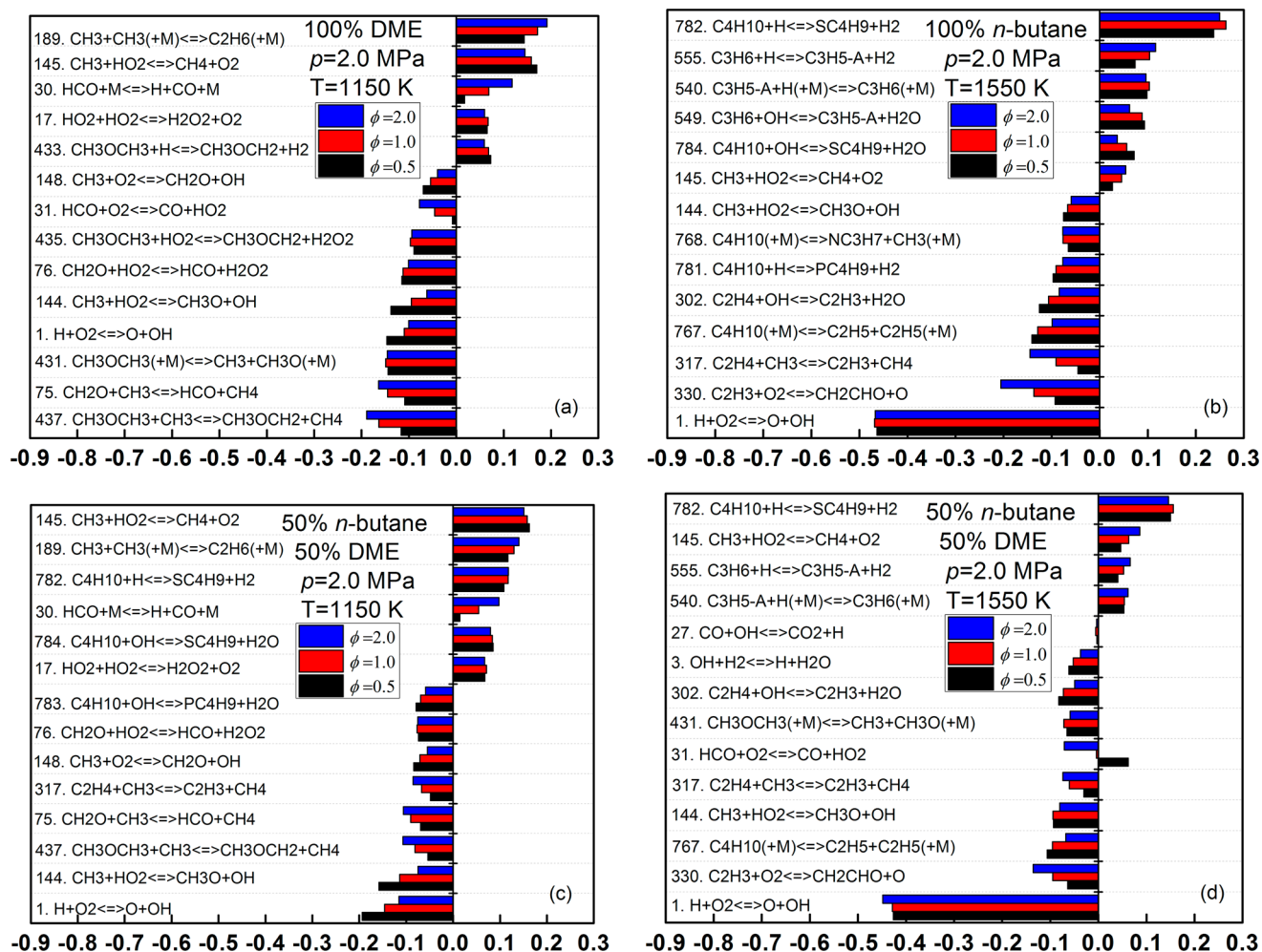


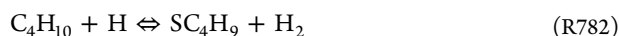
**Figure 7.** Sensitivity analysis for neat DME, neat *n*-butane, and their blends at different equivalence ratios: (a) neat DME (1150 K), (b) neat *n*-butane (1550 K), (c) 50% DME/50% *n*-butane blend (1150 K), and (d) 50% DME/50% *n*-butane blend (1550 K).

Reaction R189 is a third-order radical–radical recombination reaction, while reaction R145 is a chain termination reaction because of the productions of methane and oxygen. The sensitivity coefficient of reaction R189 is increased, and the sensitivity coefficient of reaction R145 is decreased, with the increase of the equivalence ratio because of the competition on the  $\text{CH}_3$  radical.

For neat *n*- $\text{C}_4\text{H}_{10}$  at 1550 K, as shown in Figure 7b, the most important ignition-promoting reaction is reaction R1



The most sensitive ignition-inhibiting reaction is fuel-molecule-related reaction R782.



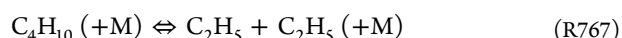
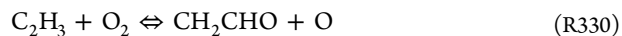
The latter produces the  $\text{SC}_4\text{H}_9$  radical via the H-abstraction reaction of *n*- $\text{C}_4\text{H}_{10}$ . It is identified that the sensitivity coefficients of reaction R1 for fuel-rich, stoichiometric, and fuel-lean mixtures are almost the same. The sensitivity coefficient of reaction R782 also shows similar behavior. Actually, for the *n*- $\text{C}_4\text{H}_{10}$  mixture, the mole fraction of oxygen varies very little with the variation of the equivalence ratio, from 4.134% under fuel-lean conditions to 3.945% under fuel-rich conditions, as shown in Table 1. This leads to the insensitivity of the ignition delay time to reaction R1. However, the mole

fraction of *n*- $\text{C}_4\text{H}_{10}$  presents an obvious change, from 0.318% under fuel-lean conditions to 1.234% under fuel-rich conditions. As a result, insufficient oxygen is available for the consumption of *n*- $\text{C}_4\text{H}_{10}$ , leading to the decreased global reaction rate and increased ignition delay time with the increase of the equivalence ratio.

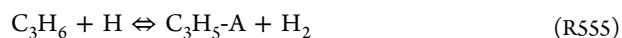
Sensitivity analyses of the 50% DME/50% *n*- $\text{C}_4\text{H}_{10}$  blend at 1150 and 1550 K are given in panels c and d of Figure 7. It was observed that the characteristic of the 50% DME/50% *n*- $\text{C}_4\text{H}_{10}$  blend combines the characteristics of neat DME at a relatively low temperature and neat *n*- $\text{C}_4\text{H}_{10}$  at a high temperature. At 1150 K, the dominant promoting reactions are reactions R1, R75, R144, and R437



and chain-branching reactions R145 and R189 are the key inhibiting reactions. This is similar to that of neat DME. At a temperature of 1550 K, the dominant promoting reactions are reactions R1, R330, and R767



while reactions R145, R555, and R782





are the main ignition-inhibiting reactions. This is similar to that of neat  $n\text{-C}_4\text{H}_{10}$ . The result from sensitivity analysis is also consistent with the experiments (Figure 4c).

**4.3. Mole Fraction Analysis of Small Radicals.** As analyzed above, the DME addition exhibits the most remarkable ignition-promoting effect on  $n\text{-C}_4\text{H}_{10}$  under fuel-rich conditions, as shown in Figure 3. Here, mole fraction analysis of small radicals was made to further interpret the ignition kinetic interaction mechanism with DME addition under fuel-rich conditions.

It is well-known that the free radicals, such as H, O, OH, and  $\text{HO}_2$ , are the important radicals for the ignition and oxidation of DME and  $n\text{-C}_4\text{H}_{10}$ . Additionally, the  $\text{CH}_3$  radical is the major production during the oxidation of DME and pyrolysis of  $n\text{-C}_4\text{H}_{10}$ . Figure 8 gives the kinetic-obtained mole fractions of small radicals, including H, O, OH,  $\text{HO}_2$ , and  $\text{CH}_3$ , yielded from neat DME, neat  $n\text{-C}_4\text{H}_{10}$ , and DME/ $n\text{-C}_4\text{H}_{10}$  fuel blends at 1150 K and 2.0 MPa. Results demonstrate that OH and H radicals are more quickly formed during the ignition induction time of DME compared to that of  $n\text{-C}_4\text{H}_{10}$ . Reaction flux analysis for  $n\text{-C}_4\text{H}_{10}$  clearly demonstrates that  $n\text{-C}_4\text{H}_{10}$  mainly undergoes the H-abstraction reactions with H and OH radicals. Therefore, fast formation of active free radicals produced from DME addition promotes the oxidation of  $n\text{-C}_4\text{H}_{10}$ .

Figures 9 and 10 show mole fractions of species, including H, OH, and  $\text{CH}_3$ , for neat DME and neat  $n\text{-C}_4\text{H}_{10}$ , respectively, at three equivalence ratios. For DME, at 1150 K, as shown in Figure 9, the dominant reaction pathway is the H-abstraction reaction with OH and  $\text{CH}_3$  radicals, accounting for 94% of the total DME consumption. During the induction time, the concentrations of  $\text{CH}_3$  and OH radicals in the fuel-rich mixture develop faster than those in the stoichiometric mixture, while those in the fuel-lean mixture give the slowest growth. As a result, richer  $\text{CH}_3$  and OH radicals in the fuel-rich mixture promote the oxidation of DME and induce faster ignition.

For neat  $n\text{-C}_4\text{H}_{10}$  at 1550 K, the H-abstraction reaction is the main consumption pathway of  $n\text{-C}_4\text{H}_{10}$ , accounting for 67% of the total consumption, and H radicals play a major role. Direct pyrolysis is another important pathway for  $n\text{-C}_4\text{H}_{10}$  consumption, where the  $\text{CH}_3$  radical is formed. Therefore, mole fractions of H and  $\text{CH}_3$  radicals are analyzed for  $n\text{-C}_4\text{H}_{10}$ , as shown in Figure 10. During induction time, an increase of the initial H concentration in the fuel-lean mixture is the fastest, while that in the fuel-rich mixture is the slowest. This leads to the increase of the ignition delay time with the increase of the equivalence ratio. However, for the  $\text{CH}_3$  radical, the concentration appears as a dual-peak characteristic. In general, the effect of the equivalence ratio on the mole fraction of the  $\text{CH}_3$  radical is negligible.

## 5. CONCLUSION

Ignition delay times of DME/ $n\text{-C}_4\text{H}_{10}$  fuel blends at various equivalence ratios and a pressure of 2.0 MPa were measured using a shock tube. A kinetic study was made to interpret the effects of the equivalence ratio and DME addition on the ignition kinetics of  $n\text{-C}_4\text{H}_{10}$  and DME. The main conclusions are summarized as follows: (1) The ignition delay times simulated using the NUIG Aramco Mech 1.3 are in good agreement with those of the measurement. (2) DME addition significantly promotes the ignition of  $n\text{-C}_4\text{H}_{10}$  under fuel-stoichiometric and fuel-rich conditions and provides a small influence of the ignition under fuel-lean conditions. DME,  $n\text{-C}_4\text{H}_{10}$ , and their blends present the same global activation

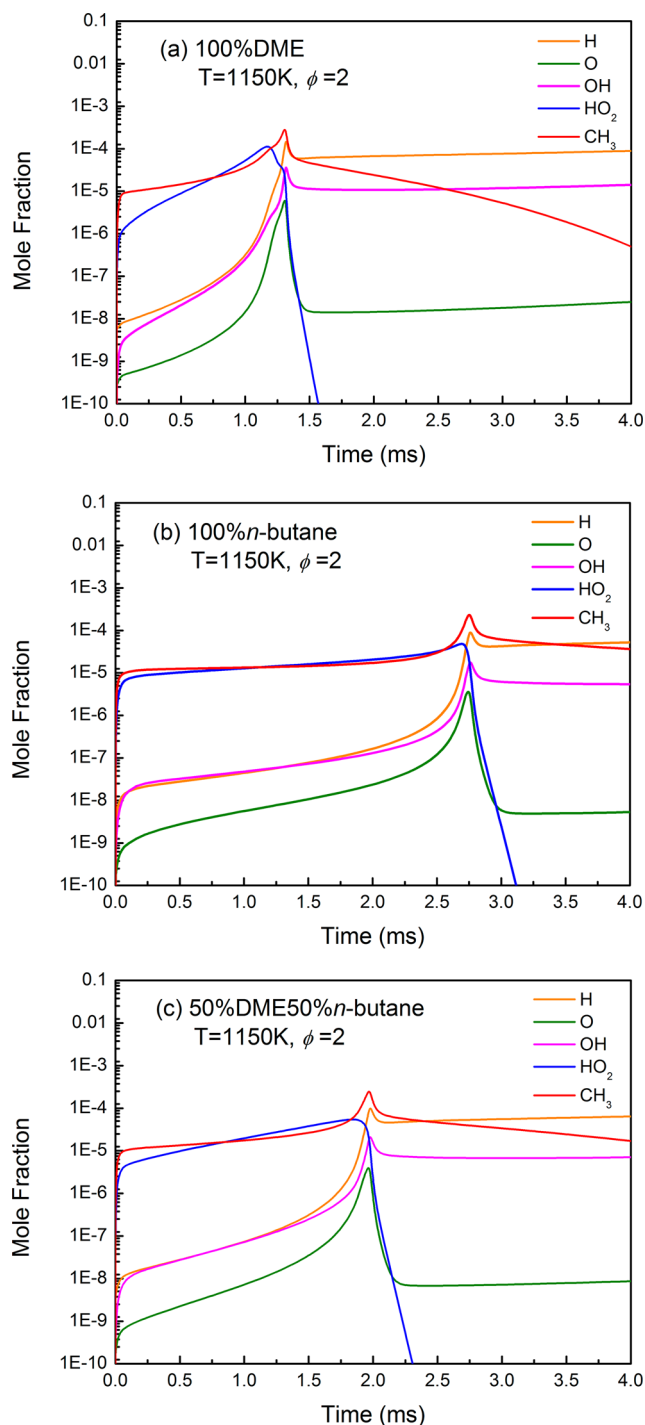


**Figure 8.** Mole fractions of free radicals and  $\text{CH}_3$  radical for neat DME, neat  $n$ -butane, and DME/ $n$ -butane fuel blends at  $\phi = 2.0$ ,  $T = 1150$  K, and  $p = 2.0$  MPa: (a) neat DME, (b) neat  $n$ -butane, and (c) 50% DME/50%  $n$ -butane blend.

energy at a given equivalence ratio. (3) The ignition delay time of neat  $n\text{-C}_4\text{H}_{10}$  increases with the increase of the equivalence ratio, and the inhibiting effect is exhibited more remarkably at high temperatures. For neat DME, the influence from the equivalence ratio is opposite that of  $n\text{-C}_4\text{H}_{10}$ . The ignition is promoted with the increase of the equivalence ratio, especially at relatively low temperatures. Ignition delay times of the 50% DME/50%  $n\text{-C}_4\text{H}_{10}$  blend show similar equivalence ratio dependency to that of neat  $n\text{-C}_4\text{H}_{10}$  at higher temperatures

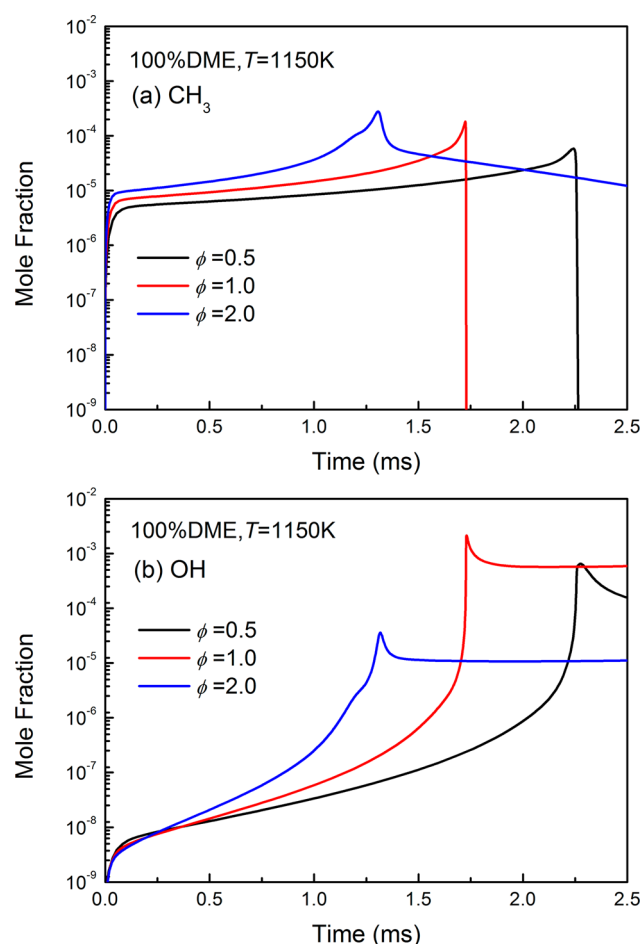


**Figure 9.** Mole fractions of OH radicals and  $\text{CH}_3$  radical for 100% DME at different equivalence ratios,  $T = 1150 \text{ K}$ , and  $p = 2.0 \text{ MPa}$ : (a)  $\text{CH}_3$  mole fraction and (b) OH mole fraction.

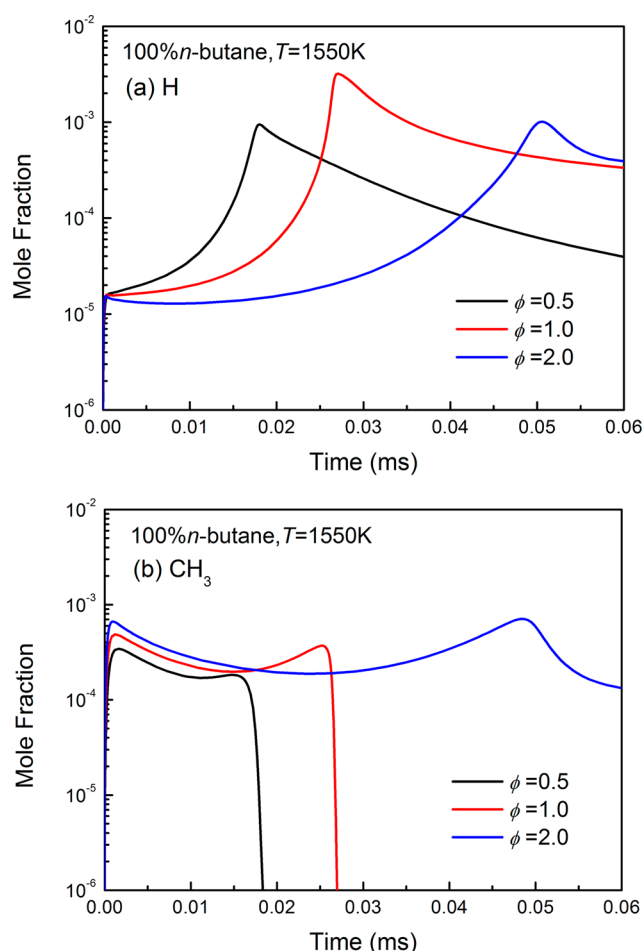


**Figure 10.** Mole fractions of H radicals and  $\text{CH}_3$  radical for 100% *n*-butane at different equivalence ratios,  $T = 1550 \text{ K}$ , and  $p = 2.0 \text{ MPa}$ : (a) H mole fraction and (b)  $\text{CH}_3$  mole fraction.

and to that of neat DME at lower temperatures. (4) DME consumption mainly undergoes the H-abstraction reaction at high temperatures, and the direct pyrolysis reaction of DME to form the  $\text{CH}_3$  radical is also important. *n*-Butane consumption mainly undergoes the H-abstraction reaction, especially with H and OH radicals. Sensitivity analysis reveals that the ignition delay time is most sensitive to the fuel related to reaction  $\text{CH}_3\text{OCH}_3 + \text{CH}_3 \rightleftharpoons \text{CH}_3\text{OCH}_2 + \text{CH}_4$  (R437) for DME at 1150 K, and the reaction rate is increased with the increase of the equivalence ratio. The most sensitive reaction is chain-branching reaction  $\text{H} + \text{O}_2 \rightleftharpoons \text{O} + \text{OH}$  (R1), and the sensitivity coefficient of this reaction does not change with the variation of the equivalence ratio. For the 50% DME/50% *n*- $\text{C}_4\text{H}_{10}$  blend, the sensitivity is similar to that of *n*- $\text{C}_4\text{H}_{10}$  at high temperatures and to that of DME at relatively low temperatures. Small radical analysis suggests that more quick formations of OH and H radicals from DME during the induction time promote the ignition of *n*- $\text{C}_4\text{H}_{10}$ . For DME at 1150 K, the increase of the equivalence ratio increases mole fractions of OH and  $\text{CH}_3$  radicals, resulting in the decreased ignition delay time. For *n*- $\text{C}_4\text{H}_{10}$  at 1550 K, the increase of the equivalence ratio decreases the mole fraction of free radical H, resulting in the increased ignition delay time.

## ■ ASSOCIATED CONTENT

### Supporting Information

All experimental data of ignition delay times of *n*-butane/DME. This material is available free of charge via the Internet at <http://pubs.acs.org>.

## ■ AUTHOR INFORMATION

### Corresponding Authors

\*Telephone: 86-29-82665075. Fax: 86-29-82668789. E-mail: yjzhang\_xjtu@mail.xjtu.edu.cn.

\*Telephone: 86-29-82665075. Fax: 86-29-82668789. E-mail: zhhuang@mail.xjtu.edu.cn.

### Notes

The authors declare no competing financial interest.

## ■ ACKNOWLEDGMENTS

This work is supported by the National Natural Science Foundation of China (51206132, 51136005, and 51121092), the National Basic Research Program (2013CB228406), and the China Postdoctoral Science Foundation (2013T60876). The authors also appreciate the funding support from the Fundamental Research Funds for the Central Universities and State Key Laboratory of Engines (SKLE201305).

## ■ REFERENCES

- (1) Arcoumanis, C.; Bae, C.; Crookes, R.; Kinoshita, E. The potential of dimethyl ether (DME) as an alternative fuel for compression-ignition engines: A review. *Fuel* **2008**, 87 (7), 1014–1030.
- (2) Dagaut, P.; Daly, C.; Simmie, J. M.; Cathonnet, M. The oxidation and ignition of dimethyl ether from low to high temperature (500–1600 K): Experiments and kinetic modeling. *Symp. (Int.) Combust., [Proc.]* **1998**, 27 (1), 361–369.
- (3) Dagaut, P.; Boettner, J. C.; Cathonnet, M. Chemical kinetic study of dimethyl ether oxidation in a jet stirred reactor from 1 to 10 ATM: Experiments and kinetic modeling. *Symp. (Int.) Combust., [Proc.]* **1996**, 26 (1), 627–632.
- (4) Cook, R. D.; Davidson, D. F.; Hanson, R. K. Shock tube measurements of ignition delay times and OH time-histories in dimethyl ether oxidation. *Proc. Combust. Inst.* **2009**, 32, 189–196.
- (5) Pfahl, U.; Fieweger, K.; Adomeit, G. Self-ignition of diesel relevant hydrocarbon air mixtures under engine conditions. *Proc. Combust. Inst.* **1996**, 26 (1), 781–789.
- (6) Hidaka, Y.; Sato, K.; Yamane, M. High-temperature pyrolysis of dimethyl ether in shock waves. *Combust. Flame* **2000**, 123 (1–2), 1–22.
- (7) Ji, C. W.; Liang, C.; Wang, S. F. Investigation on combustion and emissions of DME/gasoline mixtures in a spark-ignition engine. *Fuel* **2011**, 90 (3), 1133–1138.
- (8) Jeon, J.; Bae, C. The effects of hydrogen addition on engine power and emission in DME premixed charge compression ignition engine. *Int. J. Hydrogen Energy* **2013**, 38 (1), 265–273.
- (9) Tsutsumi, Y.; Hoshina, K.; Iijima, A.; Shoji, H. Analysis of the combustion characteristics of a HCCI engine operating on DME and methane. *SAE [Tech. Pap.]* **2007**, DOI: 10.4271/2007-32-0041.
- (10) Konno, M.; Chen, Z. Ignition mechanisms of HCCI combustion process fueled with methane/DME composite fuel. *SAE [Tech. Pap.]* **2005**, DOI: 10.4271/2005-01-0182.
- (11) Iida, N.; Yoon, H. Combustion research on internal combustion engine focus on homogeneous charge compression ignition. *SAE [Tech. Pap.]* **2009**, DOI: 10.4271/2009-32-0189.
- (12) Ohmura, T.; Ikemoto, M.; Iida, N. A study on combustion control by using internal and external EGR for HCCI engines fuelled with DME. *SAE [Tech. Pap.]* **2006**, DOI: 10.4271/2006-32-0045.
- (13) Kanoto, Y.; Ohmura, T.; Iida, N. An investigation of combustion control using EGR for small and light HCCI engine fuelled with DME. *SAE [Tech. Pap.]* **2007**, DOI: 10.4271/2007-01-1876.
- (14) Healy, D.; Donato, N. S.; Aul, C. J.; Petersen, E. L. *n*-Butane: Ignition delay measurements at high pressure and detailed chemical kinetic simulations. *Combust. Flame* **2010**, 157 (8), 1526–1539.
- (15) Zhang, J. X.; Hu, E. J.; Zhang, Z. H.; Pan, L.; Huang, Z. H. Comparative study on ignition delay times of C1–C4 alkanes. *Energy Fuels* **2013**, 27 (6), 3480–3487.
- (16) Gersen, S.; Mokhov, A. V.; Darmeveil, J. H.; Levinsky, H. B. Ignition properties of *n*-butane and iso-butane in a rapid compression machine. *Combust. Flame* **2009**, 157 (2), 240–245.
- (17) Hu, E. J.; Jiang, X.; Huang, Z. H.; Zhang, J. X. Experimental and kinetic studies on ignition delay times of dimethyl ether/*n*-butane/O<sub>2</sub>/Ar mixtures. *Energy Fuels* **2013**, 27 (1), 530–536.
- (18) Jiang, X.; Zhang, Y.; Man, X.; Pan, L.; Huang, Z. H. Shock tube measurements and kinetic study on ignition delay times of lean DME/*n*-butane blends at elevated pressures. *Energy Fuels* **2013**, 27 (10), 6238–6246.
- (19) Zhang, Y. J.; Huang, Z. H.; Wei, L. J.; Zhang, J. X. Experimental and modeling study on ignition delays of lean mixtures of methane, hydrogen, oxygen, and argon at elevated pressures. *Combust. Flame* **2012**, 159 (3), 918–931.
- (20) Zhang, J. X.; Niu, S. D.; Zhang, Y. J.; Tang, C. L. Experimental and modeling study of the auto-ignition of *n*-heptane/*n*-butanol mixtures. *Combust. Flame* **2013**, 160 (1), 31–39.
- (21) Morley, C. *Gaseq: A Chemical Equilibrium Program for Windows*; <http://www.c.morley.dsl.pipex.com/>.
- (22) Herzler, J.; Naumann, C. Shock-tube study of the ignition of methane/ethane/hydrogen mixtures with hydrogen contents from 0% to 100% at different pressures. *Proc. Combust. Inst.* **2009**, 32, 213–220.
- (23) Lutz, A. E.; Kee, R. J.; Miller, J. A. *Senkin: A Fortran Program for Predicting Homogeneous Gas Phase Chemical Kinetics with Sensitivity Analysis*; Sandia National Laboratories: Albuquerque, NM, 1987; Report SAND87e8248.
- (24) Kee, R. J.; Rupley, F. M.; Miller, J. A. *Chemkin II*; Sandia National Laboratories: Albuquerque, NM, 1989; Report 89-8009.
- (25) Metcalfe, W. K.; Burke, S.; Ahmed, S. S.; Curran, H. J. A hierarchical and comparative kinetic modeling study of C<sub>1</sub>–C<sub>2</sub> hydrocarbon and oxygenated fuels. *Int. J. Chem. Kinet.* **2013**, 45, 638–675.
- (26) Black, G.; Curran, H. J.; Pichon, S.; Simmie, J. M. Bio-butanol: Combustion properties and detailed chemical kinetic model. *Combust. Flame* **2010**, 157 (2), 363–373.
- (27) Healy, D.; Donato, N. S.; Aul, C. J.; Petersen, E. L.; Zinner, C. M.; Bourque, G.; Curran, H. J. *n*-Butane ignition delay time measurements at high pressure and detailed chemical kinetic modeling. *Combust. Flame* **2010**, 175 (8), 1526–1539.